Observations on the W-transport in the Core Plasma of JET and ASDEX Upgrade

T. Pütterich[1], R. Dux[1], R. Neu[1,2], M. Bernert[1], M.N.A. Beurskens[3] , V. Bobkov[1], S. Brezinsek[4], C. Challis[3], J.W. Coenen[4], I. Coffey[5], A. Czarnecka[6], C. Giroud[3], P. Jacquet[3], E. Joffrin[7], A. Kallenbach[1], M. Lehnen[4], E. Lerche[8], E. de la Luna[9], S. Marsen[10], G. Matthews[3], M.-L. Mayoral[2,3], R.M. McDermott[1], A. Meigs[3], J. Mlynar[11], M. Sertoli[1], G. van Rooij[12], the ASDEX Upgrade Team and JET EFDA Contributors‡

JET-EFDA, Culham Science Centre, Abingdon, OX14 3DB, UK
[1]Max-Planck-Institut für Plasmaphysik, EURATOM Assoc., 85748 Garching, Germany
[2]EFDA CSU, Boltzmannstr. 2, 85748 Garching, Germany
[3]EURATOM CCFE Fusion Assoc., Culham Science Centre, Abingdon, Oxon OX14 3DB, UK
[4]Institute of Energy- and Climate Research, Forschungszentrum Jülich, Association EURATOM-FZJ, Germany
[5]Queen's University Belfast, University Road, Belfast BT7 1NN, Northern Ireland, UK
[6]EURATOM Assoc., Inst Plasma Phys & Laser Microfus, PL-01497 Warsaw, Poland
[7]CEA, Assoc. EURATOM-CEA, IRFM, Cadarache 13108 Saint Paul Lez Durance, France
[8]Association EURATOM-Etat Belge, ERM-KMS, Brussels, Belgium
[9]EURATOM CIEMAT Assoc., Lab Nucl Fus, Madrid, Spain
[10]Max-Planck-Institut für Plasmaphysik, EURATOM Assoc., D-17491 Greifswald, Germany
[11]Association Euratom-IPP.CR, Institute of Plasma Physics AS CR, 18200 Prague, Czech Rep.
[12]DIFFER, Assoc. EURATOM-FOM, 3430BE Nieuwegein, Netherlands

E-mail: Thomas.Puetterich@ipp.mpg.de

Abstract. The W-transport in the core plasma of JET is investigated experimentally by deriving the W-concentration profiles from the modelling of the signals of the soft X-ray cameras. For the case of pure neutral beam heating W accumulates in the core ($r/a < 0.3$) approaching W-concentrations of 10^{-3} in between the sawtooth crashes, which flatten the W-profile to a concentration of about $3 \cdot 10^{-5}$. When central ICRH heating is additionally applied the core W-concentration decays in phases that exhibit a changed mode activity, while also the electron temperature increases and the density profile becomes less peaked. The immediate correlation between the change of MHD and the removal of W from the plasma core supports the hypothesis that the change of the MHD activity is the underlying cause for the change of transport. Furthermore, a discharge from ASDEX Upgrade is investigated. In this case the plasma profiles exhibit small changes only, while the most prominent change occurs in the W-content of the confined plasma caused by the reduction of the fueling deuterium gas puff. Concommintantly, the W-concentration profiles in the core plasma $r/a < 0.2$ steepen up reminescent to the well-known connection between central radiation and transport during cases with strong, established W-accumulation, while in the present analysis such a causality between the two during the onset of W-accumulation could not be

‡ See the Appendix of F. Romanelli et al., Proceedings of the 24th IAEA Fusion Energy Conference 2012, San Diego, US

pinned down. Both case studies exemplify that small changes of the core parameters of a plasma my influence the W-transport in the plasma core drastically.

1. Introduction

In ASDEX Upgrade (AUG) and JET tungsten (W) is used as a plasma facing material (cf. Ref. [1] for AUG and Ref.[2] for JET), because it will be used in ITER and it is a promising candidate material for a fusion reactor. While at AUG a stepwise approach to replacing the graphite wall tiles by W-coated ones was pursued from 1999-2007, the ITER-like wall (ILW) at JET consisting of Be (main chamber) and W (divertor) plasma facing components (PFCs) was implemented during one single vent in 2010/2011. A crucial task for plasma operation (cf. Ref. [3]) is the control of the W-concentration in the confined plasma, as W may lead to unacceptable radiative cooling for concentrations above $\approx 10^{-4}$.

A high W-content is also an issue for the stability of a plasma as plasma operation becomes more difficult when W-transport leads to a strong increase of the W-content. An extreme case of a transport phenomenon is core localized impurity accumulation. The latter is a well-known effect observed already in the limiter tokamaks PLT and ORMAK which were both operated with high-Z limiters (cf. Ref. [4, 5]). At ASDEX Upgrade and JET the operation with W PFCs is possible since the divertor concept helps to drastically reduce the W-content of the plasma [6]. However, core localized impurity accumulation is still observed in discharges where in the plasma core neoclassical transport dominates the impurity transport [7]. This happens naturally, because the profiles of density and temperature have only small gradients in the plasma core. As turbulent transport requires a threshold in the gradients of the kinetic profiles there is always a small region in the core where neoclassical transport for the impurity ions may be important, as has been shown for Ne, Ar, Kr and Xe in Ref. [8]. Neoclassical transport in the core may lead to steep impurity gradients that cause strong local radiative cooling. The easiest way of preventing impurity accumulation has been shown to be central heating by electron cyclotron resonance heating (ECRH), ion cyclotron resonance heating (ICRH) or neutral beam heating [9]. The effectiveness of this approach has been attributed to an increased turbulence level, rendering the neoclassical transport less important. The analyses of impurity transport (Si, Ar and Ni) for cases with central heating compared to cases without central heating in AUG [9, 10] and JET [11, 12] give larger diffusion coefficients and a reduction or even reversal of the convective velocity (cf. Ref.[9, 10]). In the next section a recently developed diagnostic method [13], which provides W-concentration profiles by modelling the soft X-ray emissions, is exploited in order to investigate further the transport of W in the core plasma of JET-ILW. Note that the actual work is the first at JET that focuses on W. As there is a strong Z-dependence of neoclassical transport, the uncertainties of the evaluated neoclassical transport coefficients for W receive special attention. An analysis of a discharge at

ASDEX Upgrade is used to emphasize the large effect on W-transport for small changes of the plasma profiles.

In section 2 a detailed analysis of the W-transport in the core of JET discharges is presented, which emphasizes the importance of MHD for the central W-transport. In section 3 the correlation of W-transport and W-radiation is presented and discussed and finally, section 4 summarizes the results.

2. Core Transport of Tungsten investigated in JET

2.1. Experiment and Observations

The soft X-ray cameras at JET-ILW are used to derive the profiles of W-concentration and poloidal asymmetries due to centrifugal forces. The details of the diagnostics are described in [13]. The basic assumption that allows the determination of the W-concentration is that the low-Z impurities give rise to Bremsstrahlung, while the only other radiator is W, i.e. the radiation from Ni is negligible. The rotation velocity as derived from the poloidal in-out asymmetry provides a consistency check of that assumption. For the same rotation velocity the in-out asymmetry for W is larger than for Ni. For the measured asymmetries the derived rotation velocities for W match those measured by charge exchange recombination spectroscopy, while those derived for the assumption that Ni is the main radiator would be about a factor of two too large. Generally, this observations holds in agreement to the spectroscopic observation that Ni contributes only a minor fraction $< 10\%$ even for plasmas with the highest Ni concentrations. As adjustments of the atomic data describing the soft X-ray emissions for W have been explained in Ref.[13] the physical meaning of the results may be considered preliminary, however, future corrections of the data will not change the main thrust of this paper as most of the conclusions rely on large changes of the soft X-ray emissions, outside of the uncertainties of the adjustments.

Two discharges with a plasma current of 2 MA performed at a magnetic field of 2.7 T are compared in the following. The first discharge (pulse 83597) features ≈ 16 MW of neutral beam injection (NBI) at a central density of about $7 \cdot 10^{19}\,\mathrm{m}^{-3}$. The second, pulse 83603, is heated with 14.5MW of NBI and an additional 3.5 MW of central ICRH. The central density is about $6.5 \cdot 10^{19}\,\mathrm{m}^{-3}$. The slight difference in density appears even though the deuterium gas fueling is equal for both discharges, i.e. 10^{22}D/s.

In Fig.1(a) and (b) the W-concentrations at r/a=0.0,0.3 and 0.45 are depicted for both pulses. For 83597 (pure NBI), the core W-concentration at r/a=0.0 shows large excursions compared to the values at r/a=0.3 and 0.45. At these outer radii, the only excursion is provided by a W-event at about 15.5s, which increases the W-concentration from about $3 \cdot 10^{-5}$ to 10^{-4}. The central W-concentration varies between these values and about 10^{-3}. In Fig.1(c) and (d) the electron temperature measurements from electron cyclotron emission (ECE) channels close to the magnetic axis and close to the sawtooth inversion radius (r/a$\approx$0.33) are presented. Using these signals as indicators

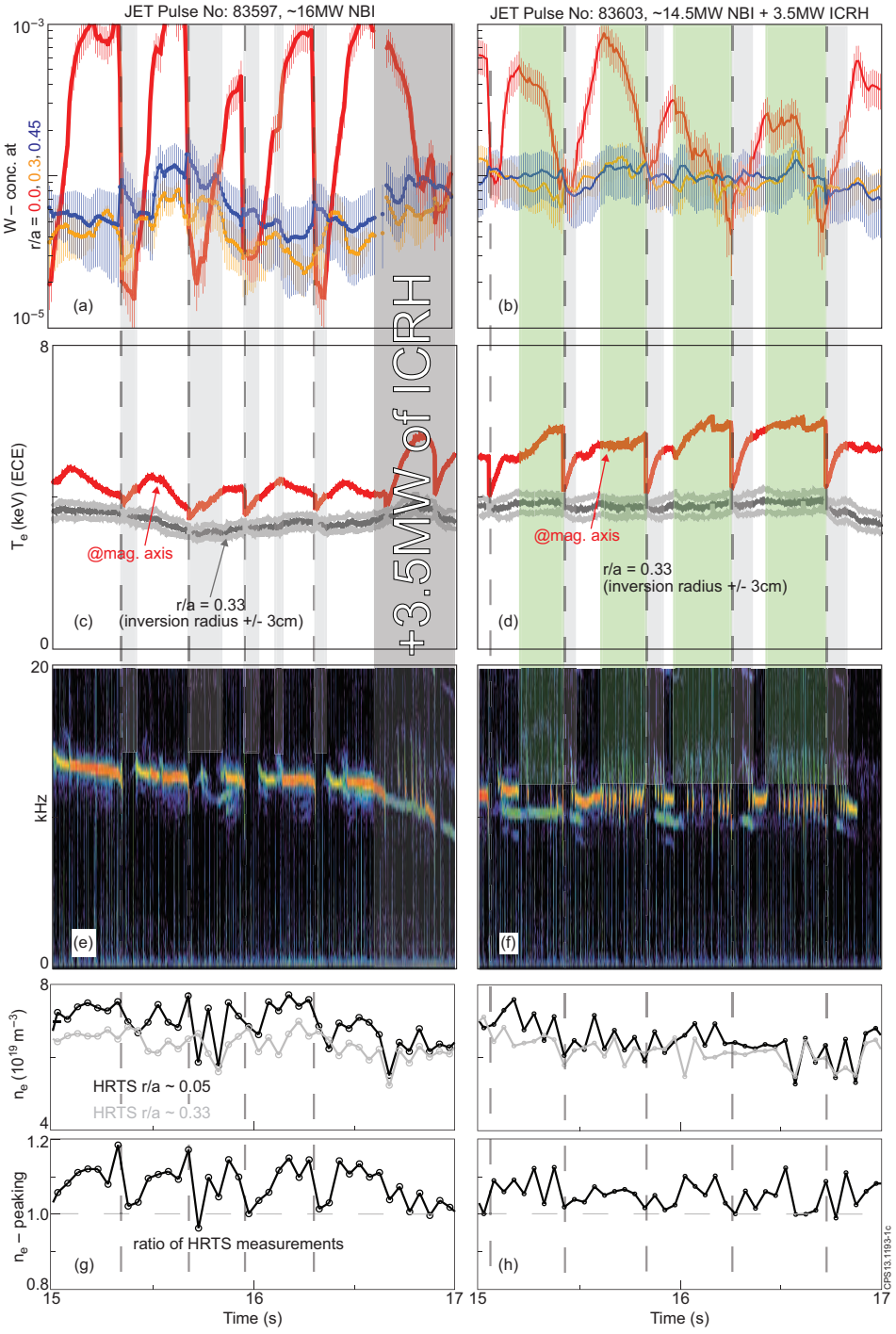

Figure 1. *(a) and (b) Evolution of the W-concentrations at three radii for 83597 and 83603; (c) and (d) Electron temperatures close to the magnetic axis and close to the sawtooth inversion radius for 83597 and 83603; (e) and (f) Spectrogram of a magnetic coil located at the outer midplane for 83597 and 83603;(g) and (h) Electron densities close to the magnetic axis and close to the sawtooth inversion radius and their ratios for 83597 and 83603;*

of the sawtooth crashes a qualitative difference between the two discharges becomes

apparent. For 83597 (pure NBI), the excursions of the W-concentration are aligned to the sawtooth crashes such that the sawtooth crash results in a flat or slightly hollow W-profile, while in the phases between the sawtooth crashes the W-concentration increases monotonically, slowly leveling off towards the end of the sawtooth cycle. For 83603 (NBI+ICRH), the W-concentration at r/a=0.3 and r/a=0.45 are slightly higher than in 83597 quantitatively consistent with the increase of the radiated power (by approx. 2 MW) from the main plasma as compared to 83597. In 83603, the increasing and decreasing phases of the central W-concentrations (at r/a=0.0) are not governed by the sawtooth cycle only. After a sawtooth crash, the W-concentration profile is flat, however, there are phases with decreasing W-concentration in between the sawteeth crashes. The interpretation of that observation is quite challenging and an attempt will be presented in the discussion section below. As an additional observation, the MHD behaviour as shown in Fig.1(e) and (f) seems to be quite different for the two pulses. For 83597 (pure NBI), a regular (1:1) mode is active during the the sawteeth cycle, while only a few perturbations of that mode activity are visible (cf. gray, transparent areas in Fig.1(a),(c) and (e)), e.g. one at 16.12 s. However, most of these special phases appear right after the sawtooth crash were density and temperature gradients are reduced, which could be the underlying reason for both, the changed transport and the changed mode activity: Right after the sawtooth crashes the mode activity is weaker and the inward transport of W pauses for about 50 to 100 ms. For 83603 (NBI+ICRH), these phases also appear after the sawtooth crashes (cf. gray, transparent areas in Fig.1(b), (d) and (f)). Apart from these, more perturbations of the MHD activity (e.g. fishbones or jumps of the frequency of the (1:1) mode) show up regularly during the sawtooth cycle (cf. green, transparent areas in Fig.1(b), (d) and (f)) and correlate with the phases in which the W-concentration in the core decreases. Simultaneously, these phases also exhibit higher electron temperatures, which could also be a cause of changed transport. In Fig.1 (g) and (h) the evolution of the electron densities in the plasma core and at the sawtooth inversion radius is shown for both discharges. Also depicted is their ratio to better diagnose the peaking of the electron density profiles. In 83597, there is a clear evolution from non-peaked to peaked within the sawtooth cycle, while in 83603 there seems to be a considerable scatter overlayed. In both cases the density ratio (core density / density at sawtooth inversion radius) is on average larger than one, thus we deal with peaked density profiles in the plasma core, while a consideration of uncertainties, as performed in the discussion section, may be crucial. The statistical uncertainties of the presented density measurements are smaller than 6 % through-out, while the propagated uncerctainties of the peaking are between 8 % and 9 % through-out.

2.2. Modelling and Discussion

In this discussion we address the following three questions:

- Is the increase of the W-concentration after a sawtooth crash in 83597 consistent with neoclassical transport or is an additional effect required?

- How strongly different is the transport in 83603?
- Is the change in MHD activity responsible for the removal of W from the plasma core in 83603?

In order to estimate the neoclassical W-transport in the plasma core a close look at the ion density and temperature profiles is necessary. The gradients of the background ions (deuterium) lead to an inward impurity convection, while the gradients in ion temperature lead to an outward convection. It should be noted that we do not attempt to do a detailed accounting of the neoclassical transport, as the uncertainties in the required measurements have a considerable effect on the neoclassical transport coefficients. The effect of these uncertainties on the W-transport is discussed below. Anyhow, the uncertainties in the electron density measurements are comparable to the change of density within a sawtooth cycle, as can be understood by looking at the time traces in Fig.1 (g) and (h). While the more regular behaviour in 83597 allows to identify a rough evolution of densities within a sawtooth cycle, it is harder to see a consistent evolution of the electron densities in 83603. For 83597, the density peaking is decreased by the sawtooth crashes and rebuilds during the sawtooth cycle. When several sawtooth cycles are taken into account, there seems to be a short phase of about 50-100ms after the sawtooth crash, where the density peaking is not reestablished or very slowly reestablished, followed by a 50-100ms phase in which the peaking is reestablished and after which the peaking saturates. Note that this is a non-negligible fraction of the sawtooth cycles, which lasts for 300-450 ms. As we plan to estimate the typical time scales of neoclassical transport we evaluate the average electron density profile including only measurements from the second half of the sawtooth cycle in which the density peaking seems to saturate. This choice neglects time-dependences and is expected to give a slightly stronger inward pinch than applies on average. For 83603, a consistent picture of the density evolution is not observed, which could mean that there is no evolution after the sawtooth crash, hence there is no peaking, or the evolution is slightly smaller than the statistical scatter of the data. In order to get at least a profile that gives us the average peaking of the densities, all time points are included in the determination of an electron density profile.

In Fig.2 the electron density profiles for the pulses 83597 and 83603 are depicted. In order to estimate the neoclassical inward convection for W, the described choice of profiles were included in the fit. For the ion temperature in the plasma core no measurement is available for large fractions of the first campaign JET with the ITER-like wall (JET-ILW). Therefore, the electron temperature measurement are used instead. At the considered high electron densities the experience of ealier campaigns at JET is suggesting that the electron temperature should be almost equal to the ion temperature, while the underlying reason for that is the fact that the typical energy exchange time is more than an order of magnitude shorter than the typical transport time. For 83603 strong localized core electron heating is provided by the ICRH, therefore, the electron temperature are considered as an upper limit for the

ion temperature. In order to make this discussion for 83603 less complex, we use, for further considerations, only one temperature profile within the phase of the sawtooth cycle, i.e. the one featuring the highest central temperatures ($\approx 6\,\mathrm{keV}$) and thus the largest outward-directed contribution for the neoclassical convection. Note that we do not attempt to do a time-dependent modelling, i.e. the transport coefficients and kinetic profiles are fixed in time (unless indicated), as the purpose of the modelling is to check the rough magnitude of the transport coefficients required to describe the observed transport phenomena. The electron temperatures measurements at the center and at the sawtooth inversion radius are presented in Fig.1 (c) and (d). The effect of impurities on the neoclassical transport coefficients is taken into account by NEOART and requires the input of impurity densities. NEOART [14, 15] calculates the collisional transport coefficients for an arbitrary number of impurities including collisions between them. The code solves the set of linear coupled equations for the parallel velocities in arbitrary toroidally symmetric geometry for all collision regimes. The classical fluxes are given by Eqs.(5.9) and (5.10) in [16]. The equations for the banana-plateau contribution are that in [17]. The Pfirsch-Schlüter contribution is calculated from the coupled equations (6.1-2) and (6.14-15) in [16], as described in [18]. The presented calculation do not take impurity asymmetries into account, which is known to alter the neoclassical transport coefficients (e.g. [19]). It should be noted that asymmetries based on centrifugal forces become less important close to the axis, while the nature of the presented analysis is that of an estimate of neoclassical transport. In the following we assume constant impurity concentration profiles (1.5% c_{Be} and 10^{-4} c_W). Both values are in the right ball park according to the data from the visible Bremsstrahlung (Be) and the soft X-ray cameras (W). Using the presented electron density profiles, the electron temperatures as measured by electron cyclotron emissions and the mentioned assumptions on impurity densities the neoclassical diffusion coefficients for W, as evaluated by NEOART, are around $0.015\mathrm{m}^2\mathrm{s}^{-1}$ for both cases (cf. Fig.2(e)and (f)). The profiles of the drift velocities for W are shown in Fig.2 (c) and (d). In both cases the most central transport is directed inward giving rise to accumulation, while at about $r/a \approx 0.15$ the drift velocity reverses and is directed outward. The outward convection is only partly due to the temperature gradients, as a bump in the density profiles between $r/a \approx 0.25$ and $r/a \approx 0.55$ gives rise to flat (83597) or slightly hollow (83603) density profile at $r/a \approx 0.2$. It is unclear if this bump is an artefact. Even though only an estimate of the neoclassical transport coefficients is attempted, we are concerned about the possible impact of such artefacts and additional complications such as the impact of gradients in the density of low-Z impurity densities which have been neglected for this analysis. These uncertainties are discussed below where also other caveats of the analysis are investigated.

For the transport modelling performed with STRAHL [14] using the atomic data derived in [20], the neoclassical transport is combined with anomalous transport, which is in the present analysis assumed ad hoc according to the results of earlier investigations on impurity transport and according to the typical impurity confinement time (s. below). In [21, 8] typical values for diffusion coefficients are found to be within the order of

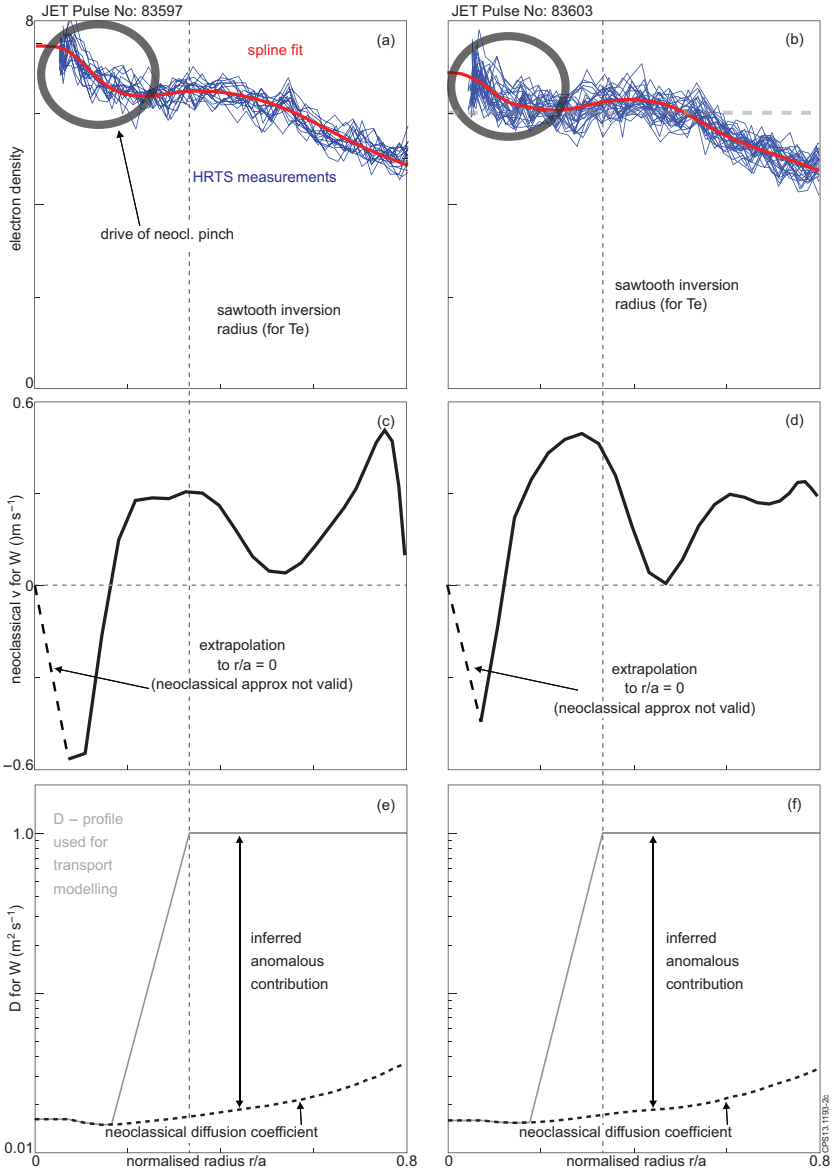

Figure 2. *(a) Density profiles as measured by HRTS during the 2nd half of the sawtooth cycles in 83597 - data (blue), spline fit (red); (b) All density profiles as measured by HRTS during the time interval 15.0 to 16.5s in 83603 - data (blue), spline fit (red); (c) Drift Velocity for W as derived from NEOART using n_e-profiles of part (a) and $T_i = T_e$ at the corresponding time points; (d) Drift Velocity for W as derived from NEOART using n_e-profiles of part (b) and $T_i = T_e$ at the end of the sawtooth cycles; (e) W-Diffusion coefficient D as used in the transport modelling and neoclassical D as derived from NEOART using n_e-profiles of part (a) and $T_i = T_e$ at the corresponding time points; (f) W-Diffusion coefficient D as used in the transport modelling and neoclassical D as derived from NEOART using n_e-profiles of part (a) and $T_i = T_e$ at the corresponding time points;*

magnitude of $1\,\mathrm{m^2 s^{-1}}$, while for cases without central heating the plasma core may exhibit neoclassical transport coefficients for impurities. As in the present work the

impurity peaking inside of r/a=0.3 is investigated the exact value of the anomalous diffusion coefficient outside of r/a=0.3 is of no importance. It is only able to influence the absolute W-concentration at r/a=0.3, which is considered a free parameter in the present study, because it can be as well influenced by the edge source and screening of the plasma, both of which are not subject of the investigations. In fact the anomalous diffusion coefficient was varied by a factor of 4 in order to confirm the insensitivity of the core analysis to the anomalous transport outside of r/a=0.3.

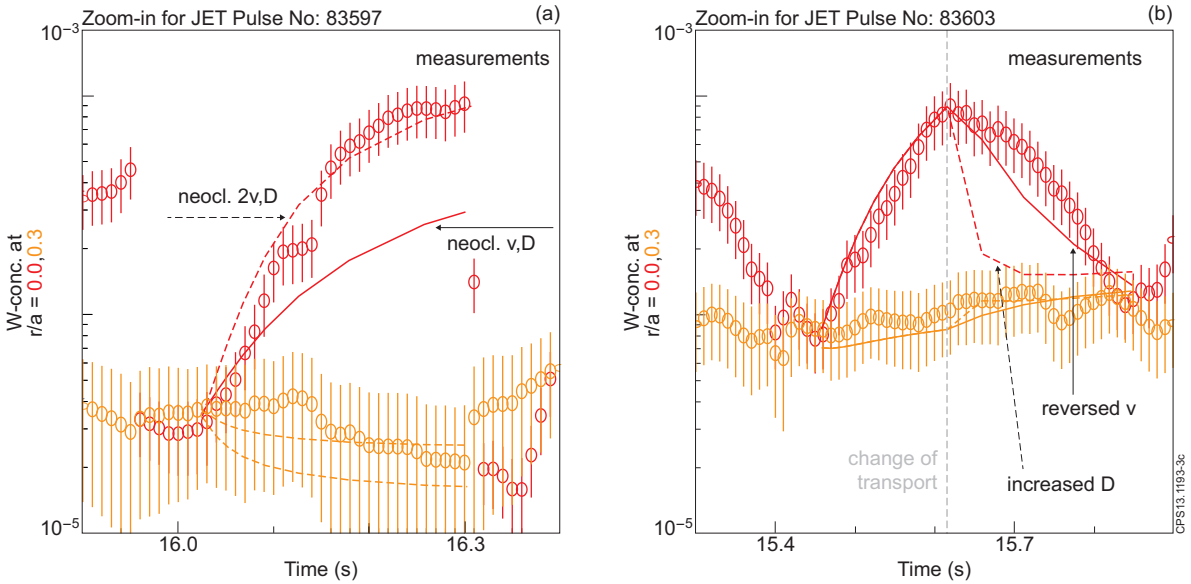

Figure 3. *(a) Zoom-in to one sawtooth cycle in 83597; The measured W-concentrations (symbols) at r/a = 0.0 (red) and r/a=0.3 (orange) are compared to modelled ones using v_{neo} and D_{neo} from neoclassical theory (solid lines) and using the v= 2· v_{neo} and D=D_{neo}. (b) Zoom-in to one sawtooth cycle in 83603; The measured W-concentrations (symbols) at r/a = 0.0 (red) and r/a=0.3 (orange) are compared to modelled ones using v and D, which are within a factor of 2 of the neoclassical coefficients up to about 15.6 s. From 15.6 s the decay of the central W-concentration is modelled by a reversed convection (solid lines) or by an increased diffusion coefficient (dashed line).*

The transition of the anomalous diffusion coefficient towards low, neoclassical values determines in which radial region the drift velocity has the biggest impact on the impurity profile. As we observe a strong W-peaking in the core only, we designed that transition region accordingly (cf. depicted diffusion coefficients in Fig.2(e) and (f)). All these adjustments are done with the aim to check the magnitude of the convective velocity and the diffusion coefficient in the region where the W-peaking is observed by comparing the time evolution of the measurements with that of the model. As mentioned above the level of the anomalous diffusion coefficients have been chosen such that approximately the impurity confinement time (few 100 ms) from experiment is reproduced and at the same time the core transport stays at the neoclassical level, while the additional W-confinement due to the W-accumulation in the plasma core was not

taken into consideration for matching impurity confinement time and level of anomalous diffusion.

Indeed, the discussed increase of the W-concentrations in the plasma core of pulse 83597 can be described (cf. Fig.3(a)) with transport coefficients reasonably close to the depicted (cf. Fig.2(c) and (e)) transport coefficients. In Fig.3(a) the results of two simulations are presented; one using exactly the transport coefficients as shown in (cf. Fig.2(c) and (e)) and one using twice the presented inward convection. The measured W-concentrations suggest that the real transport features time averaged drift velocities close to the latter coefficients. Considering the cavats, i.e. the uncertainties in the electron density profile measurements and the fact that the modelling is not time-dependent and that corrections of the neoclassical model due to centrifugal asymmetries are not taken into account, the level of agreement is surprisingly good and there is no obvious contradiction to the assumption that neoclassical transport as the main driver for the observations.

For 83603, the measurements within a sawtooth cycle cannot be described by the depicted transport coefficients, as especially the innermost part of the neoclassical transport $r/a < 0.2$ always produces a peaked profile in the core. Note that this direction of the neoclassical drift velocity is still inward even though the temperature profile featuring the highest temperatures during the sawtooth cycle are taken into account, such that the neoclassical inward convection is even stronger for most time points of the sawtooth cycle. This suggests that a change of the diffusive transport or an additional outward convection must apply in 83603, which cannot be explained by neoclassical theory. In order to document this finding the sawtooth cycle between 15.4 s and 15.8 s is modelled (cf. Fig.3(b)), while a change of transport coefficient is necessary at about 15.6 s. The increase of the W-concentration at $r/a < 0.2$ up to 15.6 s requires similar W-coefficients than for the sawtooth cycle in 83597, in detail, the core diffusion coefficient is $0.016\,\mathrm{m^2s^{-1}}$ while the convective velocity requires scaling by a factor of 2.15 such that it peaks at -0.95 $\mathrm{ms^{-1}}$. At 15.6 s the transport coefficients are changed in two different ways such that at the end of the sawtooth cycle roughly flat W-profiles result. First, the diffusion coefficient is increased to $0.5\,\mathrm{m^2s^{-1}}$ in the full region $r/a < 0.3$ and the dashed lines result in Fig.3(b). These model results feature a very steep decay of the W-concentration at $r/a = 0.0$ which then slowly approaches the flat W-profile. Second, the transport is changed in the model such that the inward convection velocity is changed from -0.95 $\mathrm{ms^{-1}}$ to an outward convection of $0.2\,\mathrm{ms^{-1}}$ in the full region $r/a < 0.3$ while the low diffusion coefficient of $0.016\,\mathrm{m^2s^{-1}}$ is maintained. These model results are shown by the solid model curves in Fig.3(b). Comparing the model curves to the data, the second model assumption seems to fit better to the data, however, if the transport coefficients are time-dependent in experiment also an increased diffusion coefficient could reproduce the measurement. In this context it is interesting to note that the neoclassical and turbulent transport is mostly governed by the kinetic profiles, which stay roughly constant between 15.55 s and 15.75 s. The modelling clearly shows that a change of transport coefficients within a sawtooth cycle is necessary to

obtain a match between the measurements and the modelling. It is not clear whether the transport coefficients are constantly changing after 15.6 s, or whether there is a simple switch of transport at 15.6s.

Both types of transport change could be caused by a change of turbulence in the plasma core or due to changed MHD activity. It is worthwhile noting that in each sawtooth cycle in 83603 the reversal of transport (i.e. from inward to outward) appears at slightly different times and combinations of central electron temperatures and densities (cf. Fig.1). The fact, that the phases with decreasing W-concentrations correlate clearly and immediately with the change in MHD activity without time lag suggests that the MHD activity could be the underlying reason for the change of the W-content, which in terms of transport coefficients may be identified as a larger anomalous diffusion coefficient or an outward drift velocity (e.g. [10, 22, 23]). The MHD activity is probably closely connected to the application of ICRH, as for example fishbone activity is known to be driven by fast particles, which may be provided by ICRH. Alternatively, the strong increase of the temperatures decreases the slowing down time of all fast particles, which leads to higher densities of fast particles, which in turn could trigger the fishbones. In [24] a similar observation is reported, as fishbones are observed to reduce the core emissivity of the soft X-ray range, which is attributed to a reduction of the core iron-density. The exact mechanism of the changed MHD activity is not subject of this study, however, it is strongly recommended to understand in more detail the mechanisms of how MHD-modes can interact with impurity transport. There are clear signs, e.g. [22, 23, 8], that not only fishbones have impact on impurity transport, but also regular (1,1)-modes. Such a future study is highly complex, because it not only has to include the mode dynamics, but also at least neoclassical impurity transport, which is very difficult to combine, as the measurements of the kinetic profiles need to be mapped onto the mode structure, which quickly rotates. Even the time-dependent treatment of the parallel redistribution of W may be a vital ingredient for perpendicular transport effects.

An alternative interpretation of the observations would be necessary, if the density peaking is much smaller than the measurements suggest (cf. discussion of caveats below). For this case no established reason for the W-accumulation in the plasma core exists, but from the obvious correlation between MHD and transport one could also conclude that the regular (1,1)-mode, which is always present during the phases which features inward transport of W, is actually causing this transport. It should be noted that such a hypothesis has several implications: There would be no clear explanation for the underlying physics of such an effect, as typically the mode activity is interpreted to cause strong, non-directional, radial transport of energy and particles. However, a change in mode-activity has been connected above and in work before (e.g. [23]) to a possible outward convection, which also cannot be described by this standard view. One should also note, that the time-scales of the increase in central W-concentrations is not compatible with v and D being both much larger than the neoclassical values (derived from the measured density peaking), thus, a directional mode transport would

by coincident result in transport of the same order of magnitude. Simulations using much larger v and D values suggest that the diffusion coefficient must be clearly smaller than $0.15\,\mathrm{m^2 s^{-1}}$ during the phases with increasing W-concentrations, while the respective v is about proportional to D. The importance of the modes cannot be excluded for the present analysis, however considering earlier high-quality work (e.g. [8]) there are clearly cases where the (1,1)-modes in the core do not play a big role for impurity transport,as it was found that neoclassical transport coefficients in the plasma core of ASDEX Upgrade apply and also exhibit a Z-dependence corresponding to that from neoclassical theory. Additionally, for the present investigation the sawtooth inversion radius, which is an indicator for the q=1 surface, is at about r/a=0.33 in 83597 and 83603, which is clearly outside of the accumulation region. Still, considering the uncertainties of the actual analysis and the incomplete understanding of interaction between modes and heavy impurities this alternative explanation can not be excluded.

2.3. Caveats

First, the derivation of the W-concentration profile from the soft X-ray cameras may be in doubt, because adjustments and recalibrations were necessary in order to use the soft X-ray cameras as a W-diagnostics. The adjustments can also be seen as a calibration procedure in order to arrive in a specific calibration discharge (without high-Z radiators) at a good description of the continuum backround radiation and in a different calibration discharge at W-concentration profiles that are consistent with bolometry and spectrometer diagnostics. The mentioned adjustments are described in more detail in Ref.[13], and for the actual discharge a consistency check is in order. As the peaking of the W-concentration is the main interest of the actual work, the question is investigated whether the diagnostic introduces a bias for the peaking and whether the considerable peaking of the W-concentration is plausible. One expectation from sawtooth crashes is that they roughly flatten all profiles, including the impurity density profiles. When comparing the W-concentrations at r/a=0.0 to the W-concentration at r/a=0.3 and r/a=0.45, the sawtooth crash indeed flatten the profiles and in a few cases even provide slightly hollow profiles (slightly outside of the error bars), which gives a hint that there might be additional uncertainties not fully captured in the error bar. On the other hand, for 83597 an impurity peaking which approaches a W-concentration of 10^{-3} just before the sawtooth is observed, which is consistent to the drop of signal in a central, horizontal chord of the bolometer system. The chord misses slightly the center of the plasma and it should be noted that due to the coarse coverage of the bolometer the neighboring chords do not detect the core localized accumulation region. The total radiated power flux on that central chords drops by $55\,\mathrm{kW\,m^{-2}}$ at the sawtooth crash. Assuming that the path length through the volume with the increased W-concentration is roughly 0.1 m (as can be derived from the signal distribution on the soft X-ray diagnostics) the average power density in the accumulation region attributed to W before the crash is thus $550\,\mathrm{kW\,m^{-3}}$, which corresponds to a change of the W-concentration of roughly

$5 \cdot 10^{-4}$ using the cooling factor from Ref. [25]. This is roughly a factor of two smaller than derived by the soft X-ray analysis, which reflects the fact that this estimate gives the average W-concentration in in the accumulation region and additionally it could be caused by the fact that the bolometer chord misses the magnetic axis by a few cm.

Second, the evaluation of the neoclassical transport coefficients for 83597 was performed taking the rough impurity densities into account, however, the influence of the impurity density profile was ignored. This was necessary, because the exact profile is unknown. Assuming that the transport is indeed neoclassical one can estimate how peaked the low-Z impurity could be. The ratio v/D describes the equilibrium impurity density profile, as in equilibrium the normalized gradient of the impurity density n_Z is given by the local ratio v_Z/D_Z. Thus, the central density peaking of an impurity Z, which may be characterized by the ratio of the impurity density at r/a=0.0 $n_Z(0.0)$ over the impurity density at r/a=0.3 $n_Z(0.3)$, is given by

$$\frac{n_Z(0.0)}{n_Z(0.3)} = exp(\int_{r@r/a=0.3}^{r@r/a=0.0} v_Z/D_Z dr)$$

, where r is the radial coordinate on which also the definition of v and D is performed. Using the obtained v and D profiles, the W-peaking in equilibrium would be about a factor of 120. As v_Z/D_Z scales to first order with the charge of the impurities, the expected v_Z/D_Z for Be, the main low-Z impurity in JET-ILW, is about a factor of 10 smaller in the plasma core. This means for the equilibrium peaking of Be that it is only a factor of 1.6. The main effect of the impurity gradients on the neoclassical transport of higher-Z elements is the reduction of the deuterium gradients, as has been shown in [26]. Thus, the relevant effect on v_W/D_W is that the deuterium gradients are reduced by less than 3.6%, as the Be-concentration peaks towards the plasma core from 1.5% to less than 2.4%. The value 2.4% is not reached, because the sawtooth crash appears before the equilibrium is reached. Thus, the estimate makes clear that the low-Z impurity gradients do not matter for the investigated discharges compared to other uncertainties.

Third, the electron density peaking in the plasma core is of similar magnitude than the density bump at mid radius, which is possibly an artefact. Still, the core localized electron density peaking is thought to be the underlying reason for the strong peaking of W-concentrations in 83597 and 83603. In 83597, the peaking is clearly real, as it features an evolution which is nicely aligned with the sawtooth cycles, however, one may wonder about the magnitude of the peaking. In 83603, the evolution is less clearly aligned with the sawtooth cycle, as is the W-concentration profile - Both suggests there is an additional effect at play, which is exactly the claim of the above discussion section. Namely the MHD activity is postulated to be important. Note that even though the density measurement is of comparably high quality, the small uncertainties affect the model results drastically, because due to the strong Z-dependence of neoclassical transport small changes in the gradient of the normalized ion densities are amplified. For an impurity charge q, the local ratio of v/D is proportional to q. For W a typical charge state in the plasma core is q=40-50. The sensitivity of the W-transport on small

changes of the background profiles is also visible in the following example from ASDEX Upgrade presented in the next section.

3. Sensitivity of Core Transport of Tungsten Investigated in ASDEX Upgrade

3.1. Experiment and Observations

Fig.4 shows time traces from an AUG discharge in which all parameters are kept as constant as possible from 3 to 6 s. The only parameter that is varied is the deuterium gas puff, which is ramped down continuously (cf. Fig.4(b)). The applied heating power is 7.5 MW of NBI and 600 kW of central ECRH (cf. Fig.4(a)). The radiated power including the divertor radiation changes from about 4 MW to 4.5 MW, while the radiated power in the main chamber increases from about 2.75 MW to 3.75 MW (cf. Fig.4(a)), which is roughly consistent with the change of the mid-radius W-concentration from $1.5 \cdot 10^{-5}$ to $3.0 \cdot 10^{-5}$ (cf. Fig.4(f)). The individual measurements of the W-concentrations are based on two different spectral emissions. The W-concentration which is attributed to mid-radius corresponds to the spectral feature at about 5 nm emitted by ion stages between W^{27+} and W^{35+}, while the central W-concentration measurement is derived from a spectral line emitted by Ni-like W^{46+} at 0.793 nm. The details of the diagnostic principle can be found in Refs. [27, 20]. Note that the bolometry cannot separate the effect of ELMs, which usually increases the bolometer signals compared to the values in between ELMs as can be derived by comparisons to fast diode measurements. The electron temperatures (cf. Fig.4(c)) and densities (cf. Fig.4(e)) do not change within the scatter of the data. This is true for the individual chords of the interferometer, and thus also for their ratio. Also, the electron temperatures close to the plasma core ($r/a \approx 0.2$) do not change. While more central measurements of the electron temperatures are not available, it is worthwhile to also consider the ion temperatures as measured by charge-exchange recombination spectroscopy (CXRS)(cf. Fig.4(e)). In order to reduce the scatter of the data the measurements have been smoothed over 4 data points (i.e. 200 ms). The ion temperature measurement at r/a=0.35 indicates a slight increase, while in the plasma core the profile is comparably flat and from $\approx$5.3 s in the discharge the difference between the core T_i-measurement (r/a=0.05) and the measurement at r/a=0.35 becomes slightly smaller indicating a reduction of the gradients. All these changes are small and are only visible after the data is smoothed, consistently no change in the stored energy derived from magnetics (W_{mhd}) is observed (cf. Fig.4(e)). The plasma rotation as measured by CXRS is also documented in Fig.4(b) and it is increasing steadily from 3 to 6 s by about 20 %, while the whole profile seems to grow consistently by about the same factor.

At about 4.8 s, an increase of W-peaking is observed (from about factor of 3 up to about a factor of 8-10, as can be derived from the ratio of the core localized W-measurement compared to the W-measurement that corresponds to about mid-radius.

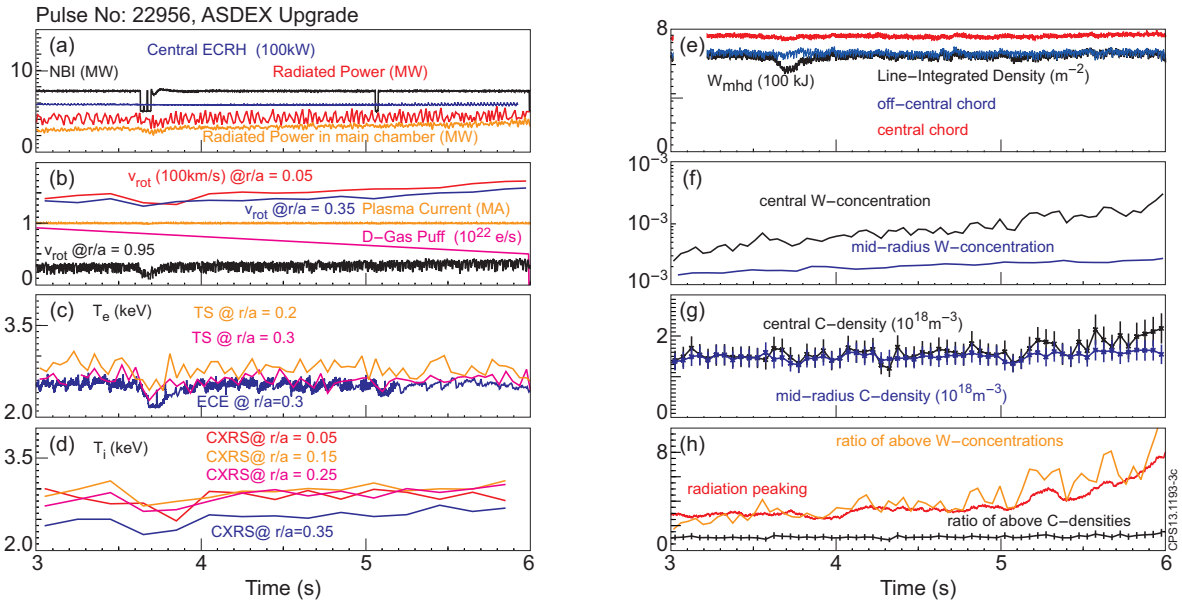

Figure 4. *Time traces for discharge # 22956 in ASDEX Upgrade. (a) Power from neutral beam injection (NBI), central electron cyclotron resonance heating (ECRH) and radiated power; (b) plasma current and deuterium gas puff for fueling; (c) Electron temperatures from Thomson scattering (TS) and electron cyclotron emission (ECE); (d) Ion temperatures (averaged over 200 ms) from charge-exchange recombination spectroscopy (CXRS); (e) Plasma stored energy (black) and line-integrated densities as measured by the DCN interferometer on a central (red) and off-central (blue) chord; (f) W-concentrations derived from spectroscopy corresponding to ion stages at mid radius and in the plasma core; (g) C-densities at mid radius and in the plasma core derived from CXRS; (h) ratio of the above W-concentrations, ratio of the above C-densities and ratio of the radiation density in the plasma core over bulk radiation density derived from bolometer chords assuming that accumulation occurs in a central region with a diameter of about 10 cm;*

In agreement to that observation, the radiation peaking increases starting at the same time (cf. Fig.4(h)). The depicted radiation ratio attributes the excess signal of a central bolometer chord to a region in the plasma core that has a diameter of about 10 cm. For considering the low-Z impurities, carbon (C) is investigated by CXRS and an interpretative code that allows for determining the C-densities from the CXRS-intensities is applied. The mid-radius C-density is changing by about 10 % from 3 to 6 s, and at about 4.8 s a slight C-peaking (up to factor of 1.4) is visible. In view of the discussion in the above sections, it should be noted that a regular (1,1)-mode exists in between sawtooth activity, very similar to the modes observed in 83597. The activity of that mode is not changing for the full time intervall considered.

3.2. Discussion

It is a common observation (e.g. [28]) that decreasing the deuterium gas puff leads to an increase of the W-content of the plasma, as the W-screening and the W-sources at

the edge are both influenced into that direction (e.g. [29, 30]). Thus, the decreasing gas puff causes the W-content at mid-radius to slowly rise. In the investigated discharge it is empirically found that the core transport also changes as can be seen by the increasing core W-concentration, which increases by a larger factor than the W-concentration at mid-radius (cf. Fig.4(e) and (f)). This effect becomes more enhanced and is well visible from 5 s onwards. It seems only parameters in the plasma core may change, while outside the only clear changes are the W-concentrations and the radiation. The interpretation of the observation is that due to the change in gas puff the edge source of W is increased which affects the radiation losses in the whole volume of the confined plasma. The radiation losses may be interpreted as negative heating power, thus, they lead to a decrease of electron temperature and its gradient. Unfortunately, the central application of ECRH prevents a central ECE measurement and the TS observation does not cover the very core of the plasma, but via heat transfer between electron and ions this effect is visible on the ion temperature which slowly and mildly decreases after 5.0 s relative to the value at r/a=0.35.

This decrease might also be so small, because the local radiation within r/a=0.2 leads to losses of about 100kW at about 5s in the discharge, while 600kW of ECRH and a few 100kW of NBI heating are deposited in the same volume. In order to understand the correlation of temperature gradients and heat flux it is necessary to quantitatively understand the turbulent state and onset thresholds for different types of turbulence. From the obtained measurements the exact causality is difficult to derive, as any effect, even the strongest one, i.e. radiation, will influence transport via the kinetic profiles which hardly change. Additionally, also rotation which is exhibiting a 20 % change may influence the core transport (cf. [31]), while typically the effect of rotation is considered small, it may become important in a situation where all changes in the plasma are small. However, it is worthwhile noting that turbulent transport is known to have a threshold in the temperature profiles, which makes a connection between temperature gradients and a strong transport change most plausible. However, the transport change takes place close to the magnetic axis (inside of r/a=0.2), where a high-quality analysis of turbulent transport is not possible due to the sensitivity of the transport codes on details of the kinetic profiles, while the measurements in the plasma core yield typically considerable uncertainties or are sparse. Note that a small change of the temperatures may affect the transport drastically, which again emphasizes the challenge to quantitatively predict and detect the conditions that lead to W-accumulation. As the transport change shows up very clearly for W and much weaker for C, a Z-scaling as observed for neoclassical transport seems to apply, which puts also an explanation in favour that describes a transition towards neoclassical transport. It should be noted that, after W-accumulation is established (not investigated here) flat or even hollow temperature profiles are observed and a change in transport (e.g. [32]) supporting the transport causing the accumulation is a well accepted fact.

Support of this transport mechanism is also provided by earlier ivestigations which documented a clear correlation between heating and transport as the core transport

could be influenced by localized heating [9]. In fact, it is rather the findings of other work (also [32]) that documented the importance of core radiation also for the onset of W-accumulation. The actual work demonstrates that the onset of W-accumulation relies on tiny changes within the confined plasma suggesting that these are encountering a threshold at which the W-transport turns instable. Note that the change of transport happens even though the radiated power is clearly much smaller than the core localized heating power giving rise to the speculation that other parameters are also playing a role.

4. Summary and Conclusions

The core transport in type-I ELMy H-modes has been investigated for JET plasmas with a plasma current of 2 MA, toroidal field of 2.7 T, a fueling gas puff of $10^{22}\,\mathrm{m}^{-3}$ and about 16MW/14.5MW of beam heating. One plasma with central ICRH has been compared to a plasma without central ICRH. The plasma without ICRH yields a strong increase of the W-concentration from about $3 \cdot 10^{-5}$ up to 10^{-3} within r/a = 0.3 during a sawtooth cycle and the sawtooth crash results in an approximately flat W-concentration profile. However, the uncertainties affect the neoclassical transport coefficients considerably, because small uncertainties in the electron measurements translate into big uncertainties for the neoclassical transport coefficients due to the strong charge dependence of the latter. When adding central ICRH the W-content of the plasma at r/a=0.45 and r/a=0.3 increases to about 10^{-4} and the central excursions of the W-concentrations become much smaller. For the same discharge the transport in between sawtooth crashes has phases which feature transport roughly consistent with neoclassical theory, but also has phases with outward transport clearly not consistent with neoclassical theory. The outward transport is best explained by an increased diffusive transport ($\approx 0.5\,\mathrm{m^2 s^{-1}}$) or a temporary outward convection ($\approx 0.2\,\mathrm{m s^{-1}}$). Due to the immediate correlation between a change of transport and a change of MHD activity (from regular (1,1)-mode to fishbones) the underlying reason for the different transport is attributed to the mode activity rather than to effects from turbulent transport or neoclassical transport. A slow change of the transport coefficients within the sawtooth cycle is also an option, still the start of the change correlates with the change in MHD.

From ASDEX Upgrade a discharge is presented in order to shed light on mechanisms that trigger W-accumulation in the core. In the discharge the heating, electron density and electron temperatures stay constant within the experimental uncertainties, while the fueling gas puff is slowly reduced. This causes a rise of the net W-influx at the edge of the confined plasma which is observed via a rise of the W-concentration at mid radius by a factor of about 2. The monitoring of the C-impurity reveals that its density at mid-radius rises only slightly and less obvious by about 10 %. At a certain time point the W-transport changes producing steeper W-concentration gradients in the plasma core, while the low-Z impurities show also weak signs of peaking, which suggests that there is a Z-dependence of transport. During this time interval the core

localized ion temperature measurement seems to be less peaked in agreement with the idea that a flattening of temperature profiles goes along with less anomalous transport, while the neoclassical transport could give rise to a Z-dependent inward transport. The changes are most obvious in the W-concentration and connected radiated power, and the W-peaking, while all other changes are close to the detection limit. The change of core transport is ultimatively achieved by the change of the plasma edge, while the plasma outside of r/a=0.2 is hardly affected at all. However, the exact causality is hard to disentangle. The most obvious change is the increasing W-concentration which may lead to a decrease in core electron temperatures, which is only visible via the ion temperature changes and which seems to be rather subtle. Possibly this causes the change of W-transport leading to the W-peaking, however there are other subtle changes happening in the plasma profiles such as rotation. As an obvious conclusion the onset of W-accumulation is identified as a process that is hard to predict, because a well stable plasma is turned into an unstable plasma, while the changes in plasma profiles are subtle.

In conclusion, the W-transport in the plasma core has been investigated and the limitations of the interpretation for both analyses exist mainly due to the fact that small changes of plasma profiles result in a large effect of the W-transport. While the driving mechanisms may be identified in today's devices, still the quantitative understanding of the transport effects are limited, e.g. for predicting the necessary mode activity to prevent W-accumulation in the core and the interaction between mode activity, turbulent transport and neoclassical transport. This also limits the predictive capabilities for future plasmas, as the prediction of the background profiles for future devices is mainly based on scaling laws.

Acknowledgement

This work was supported by EURATOM and carried out within the framework of the European Fusion Development Agreement. The views and opinions expressed herein do not necessarily reflect those of the European Commission.

References

[1] R. Neu *et al.*, Physica Scripta **T138**, 014038 (6pp) (2009).
[2] G. F. Mathews *et al.*, Journal of Nuclear Materials **438**, S2 (2013).
[3] A. Kallenbach *et al.*, Plasma Physics and Controlled Fusion **47**, B207 (2005).
[4] R. Isler, R. Neidigh, and R. Cowan, Phys. Lett. **A63**, 295 (1977).
[5] E. Hinnov and M. Mattioli, Phys. Lett. **A66**, 109 (1978).
[6] R. Neu *et al.*, Nuclear Fusion **45**, 209 (2005).
[7] R. Neu *et al.*, Journal of Nuclear Materials **313–316**, 116 (2003).
[8] R. Dux *et al.*, Nuclear Fusion **39**, 1509 (1999).
[9] R. Dux *et al.*, Plasma Physics and Controlled Fusion **45**, 1815 (2003).
[10] M. Sertoli *et al.*, Plasma Physics and Controlled Fusion **53**, 035024 (2011).
[11] M. Puiatti *et al.*, PHYSICS OF PLASMAS **13**, (2006).

[12] M. Valisa *et al.*, NUCLEAR FUSION **51**, (2011).
[13] T. Pütterich *et al.*, *Proc. of the 24rd IAEA Fusion Energy Conference, San Diego, USA* (IAEA, Vienna, 2012), Vol. IAEA-CN-197, pp. EX–P3.15.
[14] R. Dux, Technical Report No. 10/30, IPP, Garching, Germany.
[15] A. G. Peeters, provided the NEOART code, 1998.
[16] S. P. Hirshman and D. J. Sigmar, Nuclear Fusion **21**, 1079 (1981).
[17] W. A. Houlberg, K. C. Shaing, S. P. Hirshman, and M. C. Zarnstorff, Physics of Plasmas **4**, 3230 (1997).
[18] A. G. Peeters, Physics of Plasmas **7**, 268 (2000).
[19] T. Fulop and P. Helander, Physics of Plasmas **8**, 3305 (2001).
[20] T. Pütterich *et al.*, Plasma Physics and Controlled Fusion **50**, 085016 (2008).
[21] C. Giroud *et al.*, Nuclear Fusion **47**, 313 (2007).
[22] J. Stober *et al.*, in *Europhysics Conference Abstracts (CD-ROM, Proc. of the 34th EPS Conference on Plasma Physics, Warsaw, 2007)*, Vol. 31F, pp. P–5.138.
[23] M. Sertoli *et al.*, in *Europhysics Conference Abstracts (CD-ROM, Proc. of the 38th EPS Conference on Plasma Physics, Strasbourg, France, 2011)*, Vol. 35G of *ECA*, P–5.116.
[24] S. Günter *et al.*, Nuclear Fusion **39**, 1535 (1999).
[25] T. Pütterich *et al.*, Nuclear Fusion **50**, 025012 (9pp) (2010).
[26] R. Dux, Technical Report No. 10/27, IPP, Garching, Germany.
[27] R. Neu *et al.*, in *Handbook for Highly Charged Ion Spectroscopic Research*, edited by Y. Zou and R. Hutton (CRC Press, Boca Raton, FL, 2011), pp. 239–266.
[28] A. Kallenbach *et al.*, Nuclear Fusion **49**, 045007 (2009).
[29] R. Dux, A. Janzer, T. Pütterich, and ASDEX Upgrade Team, Nuclear Fusion **51**, 053002 (2011).
[30] T. Pütterich *et al.*, Journal of Nuclear Materials **415**, S334 (2011).
[31] C. Angioni, F. J. Casson, C. Veth, and A. G. Peeters, Physics of Plasmas **19**, 122311 (2012).
[32] M. Z. Tokar *et al.*, Nuclear Fusion **37**, 1691 (1997).